

Abnormally low expression of connexin 37 and connexin 43 in subcutaneously transplanted cryopreserved mouse ovarian tissue

Robert Kuo-Kuang Lee · Sheng-Hsiang Li ·
Chung-Hao Lu · Hsin-Yi Ho · Ying-Jie Chen ·
Hung-I Yeh

Received: 26 August 2008 / Accepted: 7 October 2008 / Published online: 21 October 2008
© Springer Science + Business Media, LLC 2008

Abstract

Purpose To analyze the gap junction proteins connexin 37 (Cx37) and connexin 43 (Cx43) after subcutaneous transplantation of cryopreserved mouse ovarian tissue.

Methods Expression of gap junction genes was assessed by immunohistochemistry and real-time polymerase chain reaction (PCR) in transplanted cryopreserved ovarian tissue compared with that of normal ovarian tissue. Apoptosis of ovarian cells was evaluated by using the terminal deoxynucleotidyl transferase-mediated biotinylated deoxyuridine triphosphates nick end-labeling method.

Results After subcutaneous transplantation, Cx37 and Cx43 mRNA and protein expression were significantly lower in cryopreserved than in normal ovarian tissue. Apoptosis was increased in granulosa cells from antral follicles of the cryopreserved tissue.

Conclusion After cryopreservation and subcutaneous transplantation of ovarian tissue, proteins forming gap junctions between oocytes and granulosa cells are under-expressed compared with normal controls.

Keywords Cryopreservation · Ovary · Connexin 43 · Connexin 37 · Oocyte maturation · Granulosa cell

Robert Kuo-Kuang Lee and Sheng-Hsiang Li contributed equally to this work.

Part of this work was presented at the 23rd Annual Meeting of the ESHRE in Lyon, France, 1–4 July 2007.

Capsule Abnormally low expression of Cx37 on oocytes and Cx43 on granulosa cells in subcutaneously transplanted cryopreserved mouse ovaries may contribute to failure of oocyte maturation.

R. K.-K. Lee · S.-H. Li · C.-H. Lu · Y.-J. Chen
Department of Medical Research, Mackay Memorial Hospital,
Taipei, Taiwan

H.-Y. Ho
Department of Obstetrics and Gynecology,
Mackay Memorial Hospital,
Taipei, Taiwan

H.-I. Yeh
Department of Internal Medicine,
Mackay Memorial Hospital,
Taipei, Taiwan

S.-H. Li
Nursing and Management College, Mackay Medicine,
Taipei, Taiwan

R. K.-K. Lee
Department of Obstetrics and Gynecology,
Taipei Medical University,
Taipei, Taiwan

C.-H. Lu
Institute of Biotechnology,
College of Bio-Resources and Agriculture,
National Taiwan University,
Taipei, Taiwan

R. K.-K. Lee (✉)
Department of Obstetrics and Gynecology,
Mackay Memorial Hospital,
92, Sec. 2, Chung San North Road,
Taipei 10449, Taiwan
e-mail: lsh@msl.mmh.org.tw

Introduction

Young women with cancer who are treated with chemotherapy or radiotherapy may experience infertility due to premature ovarian failure [1]. Cryopreservation of ovaries or oocytes is a potentially useful technique for storing gametes harvested from these women before their cancer treatment is begun [2–4]. Ovarian tissue banking, although still investigational, is rapidly evolving and is a promising clinical technique for preserving gonadal function. It avoids the necessity for ovarian stimulation and provides a substantial amount of tissue [5, 6]. Preservation and transplantation of the entire ovary has been reported, the advantage being immediate restoration of blood supply by vascular anastomosis [7–9]. However, ovarian tissue storage is a more practical technique [3, 6].

Successful reproduction after orthotopic transplantation or grafting into the renal capsule of cryopreserved mammalian ovaries has been demonstrated [10–12]. Human live birth after orthotopic transplantation of cryopreserved ovarian tissues has also been reported [13]. However, orthotopic or renal capsular transplantation of cryopreserved ovarian tissue is of little practical value because ovum pick up is very difficult in these locations. Subcutaneous transplantation, such as in the forearm or the abdominal wall, would solve this difficulty [6]. Follicle development is relatively easy to monitor, and the tissue is easily accessible for ovum pick up [14]. Successful fertilization and pregnancy with oocytes from subcutaneously transplanted fresh ovarian tissue have been reported in a primate [15]. In humans, a 4-cell embryo was produced from subcutaneously transplanted cryopreserved ovarian tissue, but it did not result in conception [16]. We have reported blastocyst development from cryopreserved, subcutaneously transplanted mouse ovarian tissue [17]. However, there were few good quality embryos, and successful pregnancy did not occur. In mice, graft survival was poorer and the number of oocytes retrieved was lower from subcutaneous compared with other graft sites [18]. Cryopreserved ovarian tissues are subject to freezing, thawing, and ischemic injury throughout the transplantation procedure. Grafting to a heterotopic site also potentially exposes the tissue to higher pressure or lower temperature than normal ovaries [16, 19, 20]. Presumably, these injuries impair the quality of the oocyte and subsequent embryogenesis.

In a previous study, we showed that only 25% of metaphase II oocytes could be recovered from the antral follicles of the subcutaneously transplanted cryopreserved mouse ovarian tissue, while 66% of the collected oocytes were in the germinal vesicle (GV) stage [17]. More primordial follicles die from hypoxia and delayed revascularization than from freezing-thawing injuries. The overall

result is that GV oocytes retrieved from the grafted tissue have difficulty developing into mature metaphase II oocytes, the end result being poor fertilization and pregnancy outcome. The mechanisms underlying the observed injury and dysfunction are not well understood. We designed this study to profile the expression of genes involved in the cell-cell interaction between oocytes and the surrounding granulosa cells in cryopreserved, subcutaneously transplanted mouse ovarian tissue.

Materials and methods

Animals

Specific pathogen-free outbred CD-1 mice were purchased from BioLASCO Taiwan (Taipei, Taiwan). Animals were bred in the Animal Center at the Department of Medical Research, Mackay Memorial Hospital, and were treated according to institutional guidelines for the care and use of experimental animals. They were housed under controlled lighting (14 h of light, 10 h of dark) at 21–22°C and were provided with water and chow ad libitum. Sexually mature (6–8 week-old) female mice were used for the study.

Collection of ovarian tissue

One gram of 2,2,2-tribromoethanol (Sigma-Fluka-Aldrich Chemical Co., St. Louis, MO) was dissolved in 1 mL of tertiary-amyl alcohol (J.T.Baker, Phillipsburg, NJ) to make an avertin solution for anesthesia. The mice were anesthetized with 15 $\mu\text{L/g}$ body weight of avertin solution injected intraperitoneally. Both ovaries were removed, freed of fat, and cut into three pieces each in M2 medium (Sigma) under a dissection microscope, yielding six pieces of ovarian tissue per mouse.

Freezing and thawing

We adopted the cryopreservation method of Gosden et al. [21] with some modifications. Ovarian tissue from each mouse were equilibrated at room temperature for 20 min in M2 medium containing 10% fetal bovine serum (FBS; Sigma) and 1.5 M dimethylsulfoxide (DMSO; Sigma) before being loaded into a 0.25-mL plastic freezing straw (type-2A 175; Nalge Nunc International, Rochester, NY). The straws were sealed with polyvinyl chloride powder and placed in a programmable biological freezer (CryoMed 1010, Forma Scientific Inc., Marietta, OH) at 0°C and cooled at a rate of 2°C/minutes to –7°C. They were held at –7°C for 5 min, seeded manually with previously cooled

Table 1 Collection of granulosa cells and germinal vesicle oocytes

	Batch 1		Batch 2		Batch 3	
(A). Granulosa cells for cDNA array analysis						
	Mice (n)	Cell complexes* (n)	Mice (n)	Cell complexes (n)	Mice (n)	Cell complexes (n)
Control	6	60	6	56	5	63
Cryopreserved transplant	32	63	26	48	25	50
(B). Oocytes† for real-time PCR analysis						
	Mice (n)	Cell complexes (n)	Mice (n)	Cell complexes (n)	Mice (n)	Cell complexes (n)
Control	9	115	9	110	9	108
Cryopreserved transplant	59	115	58	110	54	105

*Granulosa cells and germinal vesicle oocytes were separately collected from cell complexes after hyaluronidase treatment.

†Oocytes were collected cumulatively, thus, some oocytes came from the cell complexes listed in (A).

forceps, and held at -7°C for a further 5 min. The straws were cooled at a rate of $0.3^{\circ}\text{C}/\text{minutes}$ to -40°C and then at $10^{\circ}\text{C}/\text{minutes}$ to -150°C . They were transferred into liquid nitrogen for storage at -196°C for at least 24 h.

One day later, the cryopreserved tissues were thawed as follows. The straws were removed from liquid nitrogen, held in the air at room temperature for 20 s, and then washed twice in 2 mL of M2 medium at room temperature. After washing, the tissue was placed in M2 medium at 37°C and then immediately transplanted.

Autologous subcutaneous transplantation of cryopreserved ovarian tissue

After the mouse was anesthetized with avertin, an approximately 0.5-cm incision was made in the inguinal region, followed by blunt dissection of a 1-cm subcutaneous pocket using a pair of fine curved watchmaker's forceps. Ovarian tissue from that particular mouse was inserted into the subcutaneous space, and the skin incision was closed with a stitch of nylon suture.

Superovulation and harvesting of cells

Two weeks after grafting, the transplanted mice underwent superovulation. Pregnant mare's serum gonadotropin

(PMSG, China Chemical and Pharmaceutical Co., Hsin-Chu, Taiwan) 400 IU was injected intraperitoneally, and human chorionic gonadotropin (hCG, China Chemical and Pharmaceutical Co.), 200 IU, was given 48 h later following the previous method [17]. The mice were killed by cervical dislocation 10 h after hCG administration. The transplanted ovarian tissues were carefully removed from the inguinal areas, and oocyte-granulosa cell complexes from the antral follicles were isolated using 30-gauge needles (Becton Dickinson, Bedford, MA). After washing with M2 medium, the complexes were treated with $0.2\ \mu\text{g}/\text{ml}$ of hyaluronidase (Sigma) to separate granulosa cells and oocytes. About 66% of the oocytes from the complexes were GV-staged oocytes. The collected samples were dipped independently in PicoPure RNA extraction buffer (Arcturus Engineering, Mountain View, CA) and stored at -80°C before isolation of total RNA.

Cells were also collected from normal ovaries of 8-week-old female mice. Superovulation was stimulated with 10 IU of PMSG as above, but no hCG was given. After 48 h, the animals were killed, the oocyte-granulosa cell complexes were harvested, and the granulosa cells and GV oocytes were separated as described above. These cells were used as a control for comparing the gene expression profile of granulosa cells from subcutaneously transplanted cryopreserved ovarian tissue.

Table 2 Primer sequences

Gene ^a	Primer	Sequence	Position	Size (bp)
<i>Cx37</i>	F ^b	5'-gggcgctcatgggtacctat-3'	506~525	102
	R ^c	5'-gctccatggtccagccata-3'	607~589	
<i>Cx43</i>	F	5'-gatcgcgtgaaggaagaag-3'	867~876	101
	R	5'-cagccattgaagtaagcataatttg-3'	967~943	
<i>18S rRNA</i>	F	5'-cgagccgcctggatacc-3'	836~852	76
	R	5'-cctcagttccgaaaaccaaaa-3'	911~890	

^a GenBank accession nos.: *Cx37*, X57971; *Cx43*, X62836; *18S rRNA*, X00686. ^b F, forward primer. ^c R, reverse primer.

Table 3 Up- and down-regulated gene expression in granulosa cells from subcutaneously transplanted cryopreserved mouse ovarian tissue

Ratio*	Gene bank accession no.	Protein/Gene name	Classification
<i>Up-regulated genes</i>			
7.17	X04480	Insulin-like growth factor-IA	Growth Factor, Cytokine & Chemokine
5.86	X52264	Intercellular adhesion molecule 1 (ICAM1)	Cell Adhesion Protein
3.17	S71186	Excision repair cross-complementing rodent repair deficiency complementation group 3 (ERCC3);	Stress Response Protein
2.98	X80338	Sine oculis-related homeobox protein 2 homolog (SIX2)	Basic Transcription Factor
2.36	U77969	Neuronal PAS domain protein 2	Basic Transcription Factor
2.23	M12414	Apolipoprotein E (APOE)	Extracellular Transporter & Carrier Protein
2.15	X04648	Low-affinity IgG Fc receptor II beta (FCGR2B)	Cell Surface Antigen
2.06	U62638	Cyclin C (G1-specific)	Cyclin
<i>Down-regulated genes</i>			
36.65	M63801	Connexin 43	Cell Surface Antigen
21.09	U36340	CACCC-box-binding protein (BKLF)	Basic Transcription Factor
16.94	Z21524	Hematopoietically expressed homeobox protein (HHEX)	Basic Transcription Factor
15.66	X64361	Vav proto-oncogene	Oncogenes & Tumor Suppressors G Protein
15.49	L31609	Ribosomal protein S29 (RPS29)	Ribosomal Protein
12.30	J04806	Osteopontin (OP)	Cell Adhesion Receptor & Protein
11.80	M36829	Heat shock 84-kDa protein 1 (HSP84-1); HSP90	Heat Shock Protein
7.24	J04696	Glutathione S-transferase mu 2 (GSTM2)	Apoptosis-Associated Protein
6.50	L12140	Groucho gene-related protein (GRG)	Basic Transcription Factor
6.39	U43512	Dystroglycan 1	Matrix Adhesion Receptor
6.18	M36830	Heat shock 86-kDa protein 1 (HSP86-1); HSP90	Heat Shock Protein
5.40	M98339	GATA-binding protein 2 (GATA2)	Basic Transcription Factor
5.09	M12481	Cytoplasmic beta-actin (ACTB)	Cytoskeleton & Motility Protein
5.09	X68193	Nucleoside diphosphate kinase B (NDP kinase B; NDKB)	Oncogenes & Tumor Suppressors G Protein
5.05	X75888	G1/S-specific cyclin E1 (CCNE1)	Cyclin
5.01	AF001465	Aristaless 4 homeobox protein (ALX4)	Basic Transcription Factor
4.95	L10656	Abl proto-oncogene	Intracellular Adaptor & Receptor-Associated Protein
4.82	AJ000740	Sex-determining region Y box-containing gene 13	Basic Transcription Factor
4.71	U73488	Potassium channel, subfamily K, member 2	Membrane Channel & Transporter
4.70	X86368	Forkhead-related transcription factor 5 (FREAC5)	Basic Transcription Factor
4.59	M31131	Neural cadherin precursor (N-cadherin; CDH2)	Cell-Cell Adhesion Receptor
4.34	L21973	E2F transcription factor 1 (E2F1)	Cell Cycle Protein
4.30	Z32815	Ets-domain protein elk3	Transcription Activator & Repressor
4.25	U77714	Survival motor neuron (SMN)	Apoptosis-Associated Protein
4.21	U29762	D-binding protein (DBP)	Transcription Activator & Repressor
4.04	AF015948	E2F transcription factor 3 (E2F3)	Cell Cycle Protein
3.95	X56230	Octamer-binding transcription factor 1 (OCT1; OTF1)	Basic Transcription Factor
3.88	U12983	Cek 5 receptor protein tyrosine kinase ligand	Growth Factor, Cytokine & Chemokine
3.67	M32599	Glyceraldehyde-3-phosphate dehydrogenase (G3PDH; GADPH)	Housekeeping Gene
3.63	U65091	Melanocyte-specific gene 1 (MSG1)	Basic Transcription Factor
3.12	M30499	Myogenic factor 6 (MYF6)	Basic Transcription Factor
3.08	D26177	Leukemia inhibitory factor receptor (LIFR)	Nuclear Receptor
3.02	M83749	Cyclin D2 (CCND2)	Cyclin
2.97	L47650	Signal transducer and activator of transcription 6 (STAT6)	Transcription Activator & Repressor
2.96	U00182	Insulin-like growth factor I receptor alpha subunit (IGF-I-R alpha)	Growth Factor & Chemokine Receptor
2.88	J03770	Homeobox protein D4 (HOXD4)	Transcription Activator & Repressor
2.83	X71327	MRE-binding transcription factor	Transcription Activator & Repressor
2.76	X06746	Early growth response protein 2 (EGR2)	Basic Transcription Factor

Table 3 (continued)

Ratio*	Gene bank accession no.	Protein/Gene name	Classification
2.73	U45665	Cut-like protein 2 (CUTL2)	Basic Transcription Factor
2.54	X84814	Myotonic dystrophy locus-associated homeodomain protein homolog (DMAHP)	Basic Transcription Factor
2.51	J04115	Transcription factor AP-1	Transcription Activator & Repressor
2.50	X74342	Insulin promoter factor 1 (IPF1)	Basic Transcription Factor
2.39	D14888	Cadherin 4 (CDH4)	Cell Adhesion Receptor & Protein
2.36	U18342	Protein tyrosine kinase 3 (TYRO3)	Protein Kinase Receptor
2.35	X68837	Secretogranin II precursor (SGII)	Neuropeptide
2.27	X66032	G2/M-specific cyclin B2 (CCNB2; CYCB2)	Cyclin
2.15	S76657	cAMP response element DNA-binding protein 1 (CREBP1)	Transcription Activator & Repressor
2.13	L12705	Engrailed protein (En-2) homolog	Transcription Activator & Repressor
2.13	U19119	Interferon-inducible protein 1 (IFI1)	Transcription Activator & Repressor
2.12	U36760	Brain factor 1 (Hfbbf1)	Transcription Activator & Repressor

*Ratio of differential expression in cryopreserved transplants compared with normal ovarian granulosa cells.

cDNA array analysis of granulosa cells

For cDNA array analysis, three sample batches of granulosa cells were collected, so that the assays were performed in triplicate (Table 1). Total RNA was isolated using the PicoPure RNA isolation kit (Arcturus Engineering), and the Atlas cDNA Expression Arrays Kit (BD Biosciences Clontech, Palo Alto, CA) was used to reverse-transcribe total RNA (1.5 µg) into cDNA. The cDNA was labeled with α-³²P-dATP (NEN Life Science Products, Boston, MA) using a random primer and the labeled probes were hybridized to a nylon array (BD atlas Nylon cDNA Expression Assays, Mouse 1.2 Array, catalog no. 7853-1) in an ExpressHyb solution (BD Biosciences Clontech) at 68°

C. The membrane was exposed to a BioMax MS x-ray film (Eastman Kodak Co., Rochester, NY) with an intensifying screen at -70°C for 3 days. Relative gene expression levels were normalized by using Atlas® cDNA Expression Arrays software (BD Biosciences Clontech) according to the manufacturer's instructions. Differential expression was defined as a >2-fold difference in expression. Based on genes of interest found on this array, quantitative real-time polymerase chain reaction (PCR) was then performed.

Quantitative real-time polymerase chain reaction

Total RNA (Table 1) was extracted from GV oocytes using the PicoPure RNA isolation kit (Arcturus Engineering). A 10-µL solution was directly reverse-transcribed into a 50-µL first-strand cDNA pool using a High-Capacity cDNA Archive Kit (Applied Biosystems, Foster City, CA) according to the manufacturer's instructions. PCR primers (Table 2) were designed to cross the junction between exons and introns. We used *18S rRNA* as the internal loading control to normalize relative gene expression levels. The PCR amplification efficiency of each gene was tested to be sure it was equivalent to that of *18S rRNA* examined in a cDNA dilution series.

PCR was performed in a total volume of 20 µL, containing either 50 ng of cDNA from granulosa cells or 8 µL of cDNA from GV oocytes, 200 nM of the forward and reverse primer pair for *Cx43* (identified by cDNA array analysis as having marked differential expression in granulosa cells) and *Cx37* (on oocytes) or 25 nM of the primer pair for *18S rRNA*, and 10 µL of 2× SYBR Green Master Mix (Applied Biosystems). All reactions were performed in triplicate and run on an ABI/PRISM 7000 Sequence Detector

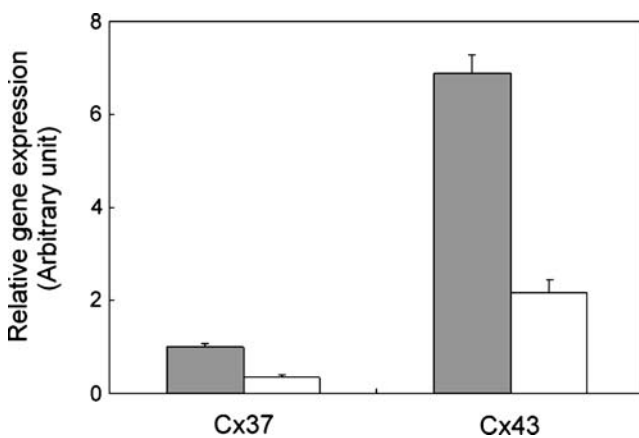


Fig. 1 Down-regulation of gap junction *Cx43* and *Cx37* mRNA in subcutaneously transplanted cryopreserved mouse ovarian tissue. Real-time PCR was used to analyze the relative expression levels of *Cx43* mRNA in granulosa cells and *Cx37* mRNA in germinal vesicle oocytes normal (light gray) and cryopreserved ovarian tissues (black)

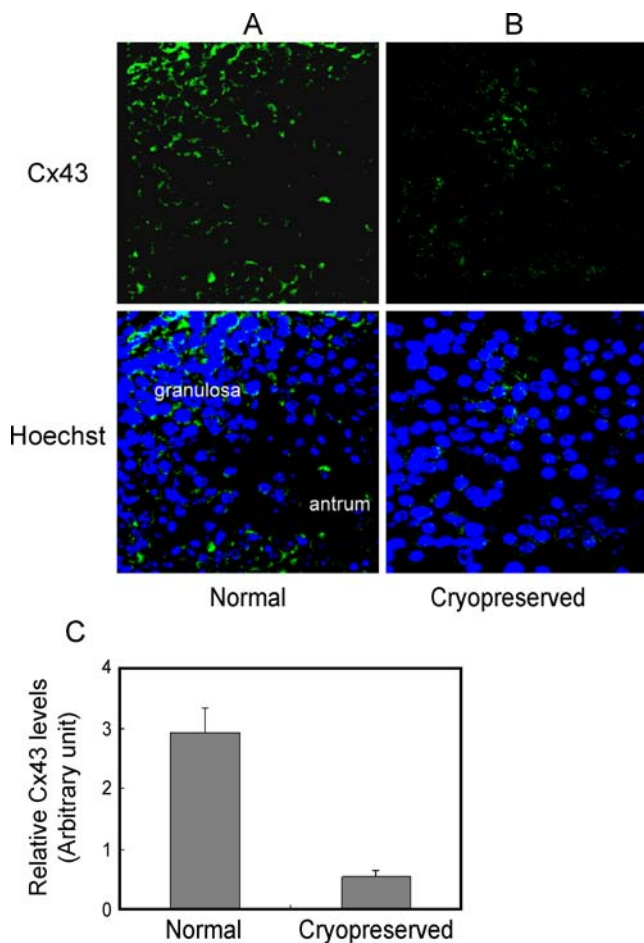


Fig. 2 Cx43 protein expression in granulosa cells. Ovarian tissues collected from normal **A** and the subcutaneously transplanted cryopreserved **B** ovarian tissues were formaldehyde-fixed, paraffin-embedded, and immunostained with anti-Cx43 antibody and FITC-conjugated secondary antibody (green). For contrast, all sections were counterstained with Hoechst 33258 for the nucleus (blue). Signals were visualized using a confocal microscope. $\times 630$. **C** Relative protein expression levels as determined by QWIN image analysis software. Data are presented as mean \pm SD

System (Applied Biosystems) under the following conditions: 50°C for 2 min, 95°C for 10 min, and then 40 cycles at 95°C for 15 s and 60°C for 1 min. The threshold cycle (Ct) was defined as the fractional cycle number at which the reporter fluorescence, i.e., the number of amplified copies, reached a fixed threshold. The melting curve was examined to verify that only a single product was formed in the reaction. The identities of the PCR products were confirmed by DNA sequencing. The relative mRNA expression levels were quantified by the $2^{-\Delta\Delta C_t}$ method [22].

Immunofluorescent localization of Cx43 and Cx37

Tissues from both transplanted and normal ovaries were fixed in a 3.7% (v/v) formaldehyde solution and embedded

in paraffin, after which 4- μ m serial cross-sections were mounted on silanated glass slides (Sigma). Deparaffinized sections were blocked with 10% (v/v) normal goat serum in phosphate-buffered saline (PBS) for 1 h at room temperature and then incubated with rabbit polyclonal anti-mouse Cx43 antibody (1:500) [23] at 4°C for overnight. GV oocytes were placed on slides and fixed in methanol for 30 s and in 3.7% paraformaldehyde for 10 min. After blocking with 10% (v/v) normal goat serum for 1 h at 37°C, the slides were incubated with rabbit polyclonal anti-mouse Cx37 antibody (1:50) [24] at 4°C for overnight.

All slides were gently agitated in three changes of PBS containing 0.1% (v/v) Tween-20 solution for 10 min each and then treated with FITC-conjugated goat anti-rabbit IgG (1:3000) (Vector Laboratories, Burlingame, CA) in 10% (v/v) normal goat serum for 1 h at room temperature. All slides were washed again as above and counterstained with Hoechst 33258 (Sigma) to mark the cell nucleus.

Slides were examined by laser scanning confocal microscopy using a Leica TCS SP equipped with an argon/krypton ion laser and UV laser with the appropriate filter spectra adjusted for the detection of FITC

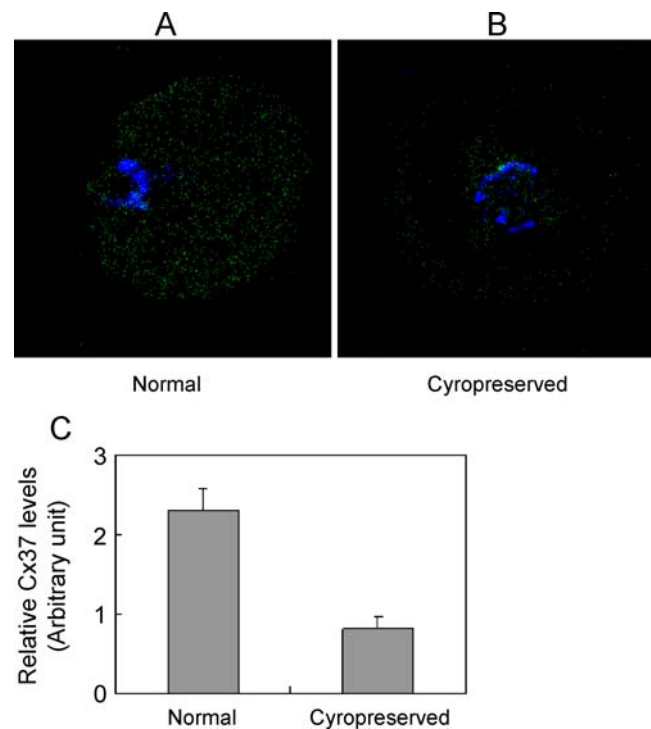
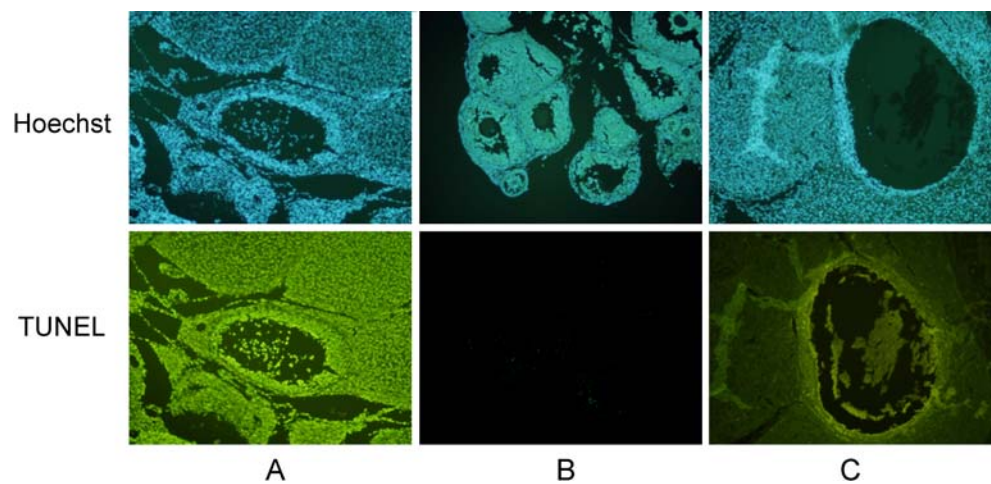


Fig. 3 Cx37 protein expression in germinal vesicle oocytes. Oocytes collected from normal **A** and subcutaneously transplanted cryopreserved **B** ovarian tissue were fixed and immunostained with anti-Cx37 antibody and FITC-conjugated secondary antibody. For contrast, all sections were counterstained with Hoechst 33258 for the nucleus (blue). Signals were visualized using a confocal microscope. $\times 630$. **C** Relative protein expression levels as determined by QWIN image analysis software. Data are presented as mean \pm SD

Fig. 4 Apoptosis of ovarian cells in normal and subcutaneously transplanted cryopreserved ovarian tissue assessed by the TUNEL method. The apoptosis signal is shown in green. The nuclear staining of Hoechst 33258 (blue) is shown for contrast. **A** Deoxyribonuclease treated positive control. **B** Staining pattern of normal control tissue. **C** Staining pattern of subcutaneously transplanted cryopreserved ovarian tissue, with extensive apoptotic death of granulosa cells. $\times 200$



(green) and Hoechst (blue) fluorescence. Quantification of Cx43- and Cx37-labeled spots was conducted using QWIN image analysis software (Leica; Heidelberg, Germany).

Apoptosis assay of ovarian tissues

Apoptosis was evaluated by using the terminal deoxynucleotidyl transferase-mediated biotinylated deoxyuridine triphosphates nick end-labeling (TUNEL) method according to the manufacture's instructions (Promega, Madison, WI).

Results

The cDNA array used to profile gene expression contains ~1200 genes, many of which are involved in follicular development. A total of 58 genes were found to be differentially expressed in transplanted cryopreserved ovarian tissue, including 50 that were down-regulated. These were genes for gap junctions, transcription factors, cell adhesion proteins, heat shock proteins, and cell cycle-related proteins. There were eight up-regulated genes in the cryopreserved transplants, including those for insulin-like growth factor I, cyclin C, and apolipoprotein E. The gap junction gene *Cx43*, encoding for a connexin involved in cell-cell interaction, was markedly down-regulated in granulosa cells from cryopreserved transplants, its differential expression deviating from normal by over 36-fold (Table 3).

Real-time PCR analysis confirmed that *Cx43* mRNA was markedly reduced in granulosa cells collected from antral follicles of cryopreserved, transplanted ovarian tissue (Fig. 1). *Cx43* protein in granulosa cells is associated with *Cx37* protein on oocytes to construct connexons which are essential for oocyte development [25]. Therefore, we examined the expression of *Cx37* mRNA in GV oocytes collected from the transplanted cryopreserved ovarian tissue. *Cx37* mRNA was significantly lower in the

cryopreserved transplants compared with normal control tissue (Fig. 1).

On immunofluorescent staining, *Cx43* protein spots were obvious on granulosa cells of normal ovary (Fig. 2A), but, although the expression did vary from slide to slide, there were markedly fewer such spots on cryopreserved, transplanted ovarian tissue (Fig 2B). Quantitative analysis of the *Cx43* proteins on slides of the transplanted tissue revealed an average 5-fold decrease from normal (Fig. 2C). Similarly, *Cx37* proteins were poorly expressed on the GV oocytes of cryopreserved transplants, the slides having an approximately 3-fold decrease from normal (Fig. 3). TUNEL analysis was performed to assess apoptosis in ovarian granulosa cells. The deoxynuclease-treated slide, the positive control, showed the positive staining to ensure the success of the experiment (Fig. 4A). Apoptosis in granulosa cells of the normal control ovarian tissue was nearly undetectable (Fig. 4B). However, increased apoptosis in granulosa cells of cryopreserved transplants was demonstrated (Fig. 4C).

Discussion

Our cDNA array data revealed abnormal gene expression in granulosa cells from antral follicles of subcutaneously transplanted cryopreserved mouse ovarian tissue. The greatest abnormality was found in a gene coding for gap junction proteins. The mRNA and protein expression of *Cx43* in granulosa cells was significantly lower than that in cells from normal ovaries. The corresponding connexin, *Cx37*, on GV oocytes was also underexpressed compared to normal. In addition, extensive apoptosis was detected in granulosa cells from the cryopreserved, transplanted ovarian tissue. Our data suggest there is impaired cell-cell adhesion or interaction between granulosa cells and oocytes in cryopreserved ovarian tissue that has been transplanted subcutaneously. This may explain, at least in part, the poor

development of follicles in such grafts, even though the oocytes themselves survive the freezing, thawing, and transplantation.

Gap junctions are aggregations of intercellular channels composed of protein connexins that directly connect adjacent cells, allowing movement of ions, metabolites, and signaling molecules from cell to cell [26]. During follicular development, a considerable volume of molecules are exchanged between granulosa cells and oocytes, including important bi-directional signals. This intercellular communication is an important facet of the development of an egg that is competent to undergo fertilization and embryogenesis [26–28].

Cx43 is the major gap junction protein produced by the granulosa cell, participating in connexons with other granulosa cells in addition to those with oocytes. Cx37 appears to be the only connexin contributed by oocytes; it forms a heterologous gap junction with granulosa cells [25]. Loss of Cx37 interferes with the development of antral follicles [26, 29]. Injury to granulosa cells may affect further folliculogenesis [19]. It has been hypothesized that poor folliculogenesis in cryopreserved ovaries is attributable to dysfunction of granulosa cells but not of oocytes [17, 30]. Previously, we have shown that oocytes survive in adequate numbers in subcutaneously transplanted cryopreserved ovarian tissue [17]. Granulosa cells are reportedly more vulnerable to ischemia than primordial follicles [31], and in this study, we demonstrated a higher than normal rate of apoptosis in granulosa cells from cryopreserved ovaries (Fig. 4). Primordial follicles, which are relatively dormant, tolerate freezing and thawing better than more developed follicles compared to other stages [31].

Navarro-Costa et al. reported disruption of granulosa cell-oocyte interface after cryopreservation [32], but they did not transplant the thawed tissue and thus could not evaluate the damage after tissue grafting. An ultrastructural study of cryopreservation and transplantation of human ovarian tissue has shown that freezing, thawing, and transplantation do not greatly affect primordial follicle ultrastructure [33]. However, the development of the oocyte and granulosa cells is asynchronous, which might result in functional uncoupling of oocytes and granulosa cells. Taken together with our results, these experiments suggest that oocytes and granulosa cells respond differently to cryopreservation and to transplantation.

It has been reported that freezing and thawing increases apoptosis in ovarian cells [34] but the molecular mechanisms of ovarian follicle apoptosis remain to be investigated. The loss of primordial follicles after grafting has been attributed mainly to ischemia and hypoxia before the grafted fragment is revascularized [17, 31, 35]. In this study, we have demonstrated that granulosa cell-oocyte interaction is damaged in tissue that has undergone

cryopreservation and subcutaneous transplantation. Indeed, there was a higher rate of apoptosis than normal in granulosa cells from transplanted tissue, but whether the increased cell death can be attributed directly to the abnormalities in gap junction proteins remains to be seen.

While subcutaneous transplantation makes ovum pick up easier, that advantage must be weighed against the risk of follicle loss from ischemia. Our study demonstrates a loss in integrity of the granulosa cell-oocyte interface after cryopreservation and subcutaneous transplantation. Follicular development is a complex process involving the coordinated growth and differentiation of oocytes and their accompanying granulosa cells. Since folliculogenesis is known to be gap-junction dependent, our findings may be useful in evaluating the integrity of granulosa-oocyte interface, perhaps providing a means of monitoring functional follicular development. Transplantation procedures need to be further optimized to minimize damage to granulosa cells in transplanted cryopreserved ovarian tissue.

Conclusions

We have demonstrated under-expression of Cx43 in granulosa cells and of Cx37 in oocytes in subcutaneously transplanted cryopreserved mouse ovarian tissues, along with increased apoptosis of granulosa cells. This leads us to speculate that the poor retrieval of mature oocytes from such grafts may in part result from the failure of signal transduction and metabolite transmission between granulosa cells and the oocyte.

Acknowledgements This work was supported by grants from the National Science Council (NSC93-2314-B-195-011) and Mackay Memorial Hospital (MMH 9408), Taipei, Taiwan.

References

1. Chambers SK, Chambers JT, Kier R, Peschel RE. Sequelae of lateral ovarian transposition in irradiated cervical cancer patients. *Int J Radiat Oncol Biol Phys.* 1991;20:1305–8.
2. Donnez J, Martinez-Madrid B, Jadoul P, Van Langendonck A, Demylle D, Dolmans MM. Ovarian tissue cryopreservation and transplantation: a review. *Hum Reprod Update.* 2006;12:519–35. doi:10.1093/humupd/dml032.
3. Shamonki MI, Oktay K. Oocyte and ovarian tissue cryopreservation: indications, techniques, and applications. *Semin Reprod Med.* 2005;23:266–76. doi:10.1055/s-2005-872455.
4. Siebzehnrubl E. Cryopreservation of ovarian tissue to preserve female fertility - state of the art. *Andrologia.* 2003;35:180–1. doi:10.1046/j.1439-0272.2003.00552_10.x.
5. Ovarian tissue and oocyte cryopreservation. *Fertil Steril.* 2006;86: S142–7.
6. Poirot CJ, Martelli H, Genestie C, Golmard JL, Valteau-Couanet D, Helardot P, et al. Feasibility of ovarian tissue cryopreservation for

- prepubertal females with cancer. *Pediatr Blood Cancer*. 2007;49:74–8. doi:10.1002/psc.21027.
7. Jadoul P, Donnez J, Dolmans MM, Squifflet J, Lengele B, Martinez-Madrid B. Laparoscopic ovariectomy for whole human ovary cryopreservation: technical aspects. *Fertil Steril*. 2007;87:971–5. doi:10.1016/j.fertnstert.2006.10.012.
 8. Martinez-Madrid B, Camboni A, Dolmans MM, Nottola S, Van Langendonck A, Donnez J. Apoptosis and ultrastructural assessment after cryopreservation of whole human ovaries with their vascular pedicle. *Fertil Steril*. 2007;87:1153–65. doi:10.1016/j.fertnstert.2006.11.019.
 9. Martinez-Madrid B, Donnez J. Cryopreservation of intact human ovary with its vascular pedicle—or cryopreservation of hemiovaries? *Hum Reprod*. 2007;22:1795–6. author reply 1796–7. doi:10.1093/humrep/dem047.
 10. Candy CJ, Wood MJ, Whittingham DG. Restoration of a normal reproductive lifespan after grafting of cryopreserved mouse ovaries. *Hum Reprod*. 2000;15:1300–4. doi:10.1093/humrep/15.6.1300.
 11. Liu J, Van der Elst J, Van den Broecke R, Dhont M. Live offspring by in vitro fertilization of oocytes from cryopreserved primordial mouse follicles after sequential in vivo transplantation and in vitro maturation. *Biol Reprod*. 2001;64:171–8. doi:10.1095/biolreprod64.1.171.
 12. Liu J, Van Der Elst J, Van Den Broecke R, Dumortier F, Dhont M. Maturation of mouse primordial follicles by combination of grafting and in vitro culture. *Biol Reprod*. 2000;62:1218–23. doi:10.1095/biolreprod62.5.1218.
 13. Donnez J, Dolmans MM, Demyelle D, Jadoul P, Pirard C, Squifflet J, et al. Livebirth after orthotopic transplantation of cryopreserved ovarian tissue. *Lancet*. 2004;364:1405–10. doi:10.1016/S0140-6736(04)17222-X.
 14. Oktay K, Economos K, Kan M, Rucinski J, Veeck L, Rosenwaks Z. Endocrine function and oocyte retrieval after autologous transplantation of ovarian cortical strips to the forearm. *JAMA*. 2001;286:1490–3. doi:10.1001/jama.286.12.1490.
 15. Lee DM, Yeoman RR, Battaglia DE, Stouffer RL, Zelinski-Wooten MB, Fanton JW, et al. Live birth after ovarian tissue transplant. *Nature*. 2004;428:137–8. doi:10.1038/428137a.
 16. Oktay K, Buyuk E, Veeck L, Zaninovic N, Xu K, Takeuchi T, et al. Embryo development after heterotopic transplantation of cryopreserved ovarian tissue. *Lancet*. 2004;363:837–40. doi:10.1016/S0140-6736(04)15728-0.
 17. Lee RK, Ho HY, Yu SL, Lu CH. Blastocyst development after cryopreservation and subcutaneous transplantation of mouse ovarian tissue. *J Assist Reprod Genet*. 2005;22:95–101. doi:10.1007/s10815-005-1499-z.
 18. Yang HY, Cox SL, Jenkin G, Findlay J, Trounson A, Shaw J. Graft site and gonadotrophin stimulation influences the number and quality of oocytes from murine ovarian tissue grafts. *Reproduction*. 2006;131:851–9. doi:10.1530/rep.1.00916.
 19. Choi J, Lee JY, Lee E, Yoon BK, Bae D, Choi D. Cryopreservation of the mouse ovary inhibits the onset of primordial follicle development. *Cryobiology*. 2007;54:55–62. doi:10.1016/j.cryobiol.2006.11.003.
 20. Wolner-Hanssen P, Hagglund L, Ploman F, Ramirez A, Manthorpe R, Thuring A. Autotransplantation of cryopreserved ovarian tissue to the right forearm 4(1/2) years after autologous stem cell transplantation. *Acta Obstet Gynecol Scand*. 2005;84:695–8. doi:10.1111/j.0001-6349.2005.00654.x.
 21. Gosden R, Newton H, Kim SS. The cryopreservation of human ovarian tissue. In: Kempers RD, Cohen J, Haney AF, Younger JB, editors. *Fertility and reproductive medicine*. Amsterdam: Elsevier; 1998. p. 615–20.
 22. Livak KJ, Schmittgen TD. Analysis of relative gene expression data using real-time quantitative PCR and the 2(-Delta Delta C (T)). *Methods Methods*. 2001;25:402–8.
 23. Yeh HI, Lai YJ, Lee YN, Chen YJ, Chen YC, Chen CC, et al. Differential expression of connexin43 gap junctions in cardiomyocytes isolated from canine thoracic veins. *J Histochem Cytochem*. 2003;51:259–66.
 24. Yeh HI, Lu CS, Wu YJ, Chen CC, Hong RC, Ko YS, et al. Reduced expression of endothelial connexin37 and connexin40 in hyperlipidemic mice: recovery of connexin37 after 7-day simvastatin treatment. *Arterioscler Thromb Vasc Biol*. 2003;23:1391–7. doi:10.1161/01.ATV.0000083508.21989.15.
 25. Kidder GM, Mhawi AA. Gap junctions and ovarian folliculogenesis. *Reproduction*. 2002;123:613–20. doi:10.1530/rep.0.1230613.
 26. Carabatsos MJ, Sellitto C, Goodenough DA, Albertini DF. Oocyte-granulosa cell heterologous gap junctions are required for the coordination of nuclear and cytoplasmic meiotic competence. *Dev Biol*. 2000;226:167–79. doi:10.1006/dbio.2000.9863.
 27. Goodenough DA, Simon AM, Paul DL. Gap junctional intercellular communication in the mouse ovarian follicle. *Novartis Found Symp*. 1999;219:226–35. discussion 235–40. doi:10.1002/9780470515587.ch14.
 28. Matzuk MM, Burns KH, Viveiros MM, Eppig JJ. Intercellular communication in the mammalian ovary: oocytes carry the conversation. *Science*. 2002;296:2178–80. doi:10.1126/science.1071965.
 29. Simon AM, Goodenough DA, Li E, Paul DL. Female infertility in mice lacking connexin 37. *Nature*. 1997;385:525–9. doi:10.1038/385525a0.
 30. Siebzehnrubl E, Kohl J, Dittrich R, Wildt L. Freezing of human ovarian tissue—not the oocytes but the granulosa is the problem. *Mol Cell Endocrinol*. 2000;169:109–11. doi:10.1016/S0303-7207(00)00362-2.
 31. Kim SS, Yang HW, Kang HG, Lee HH, Lee HC, Ko DS, et al. Quantitative assessment of ischemic tissue damage in ovarian cortical tissue with or without antioxidant (ascorbic acid) treatment. *Fertil Steril*. 2004;82:679–85. doi:10.1016/j.fertnstert.2004.05.022.
 32. Navarro-Costa P, Correia SC, Gouveia-Oliveira A, Negreiro F, Jorge S, Cidado AJ, et al. Effects of mouse ovarian tissue cryopreservation on granulosa cell-oocyte interaction. *Hum Reprod*. 2005;20:1607–14. doi:10.1093/humrep/deh787.
 33. Nottola SA, Camboni A, Van Langendonck A, Demyelle D, Macchiarelli G, Dolmans MM, et al. Cryopreservation and xenotransplantation of human ovarian tissue: an ultrastructural study. *Fertil Steril*. 2007; In press.
 34. Fauque P, Ben Amor A, Joanne C, Agnani G, Bresson JL, Roux C. Use of trypan blue staining to assess the quality of ovarian cryopreservation. *Fertil Steril*. 2007;87:1200–7. doi:10.1016/j.fertnstert.2006.08.115.
 35. Israely T, Nevo N, Harmelin A, Neeman M, Tsafiriri A. Reducing ischaemic damage in rodent ovarian xenografts transplanted into granulation tissue. *Hum Reprod*. 2006;21:1368–79. doi:10.1093/humrep/del010.